



Brazilian Journal of Physics

ISSN: 0103-9733

luizno.bjp@gmail.com

Sociedade Brasileira de Física  
Brasil

Bonilla, C. M.; Landínez Téllez, D. A.; Rodríguez Martínez, J. Arbey; Roa-Rojas, J.  
Ab Initio Study of Half-Metallic Feature and Electronic Structure of  $A_2\text{FeMoO}_6$  ( $A=\text{Ba}, \text{Ca}$ ) Magnetic  
System

Brazilian Journal of Physics, vol. 36, núm. 3B, september, 2006, pp. 1101-1104

Sociedade Brasileira de Física

São Paulo, Brasil

Available in: <http://www.redalyc.org/articulo.oa?id=46436580>

- How to cite
- Complete issue
- More information about this article
- Journal's homepage in redalyc.org

redalyc.org

Scientific Information System

Network of Scientific Journals from Latin America, the Caribbean, Spain and Portugal

Non-profit academic project, developed under the open access initiative

## ***Ab Initio* Study of Half-Metallic Feature and Electronic Structure of $A_2FeMoO_6$ (A=Ba,Ca) Magnetic System**

C. M. Bonilla\*, D. A. Landínez Téllez\*, J. Arbey Rodríguez Martínez<sup>†</sup>, and J. Roa-Rojas\*

\*Grupo De Física de Nuevos Materiales, Departamento de Física,  
Universidad Nacional de Colombia, AA 14490, Bogotá DC, Colombia

<sup>†</sup> Grupo de Física de la Materia Condensada, Departamento de Física,  
Universidad Nacional de Colombia, AA 14490, Bogotá DC, Colombia

Received on 4 December, 2005

We report several *ab initio* calculations performed over the  $A_2FeMoO_6$  (A=Ba, Ca) double perovskite. Results show that it is an insulator for the spin up orientation and conductor for the other one. We investigate the electronic structure of  $A_2FeMoO_6$  by means calculations of density of states for both spin orientations, based on the Density Functional Theory and the Linearized Augmented Plane Waves method. For the exchange correlation potential we chose the Generalized Gradient Approximation since this potential consider the difference between the electronic densities for the two distinct spin orientations from the beginning. The density of states is calculated by the histogram method and the position of the Fermi level is found by integrating over the density of states for both spin orientations. With the calculated densities of states, the half metallic properties of these compounds can be observed with the position of the Fermi level. Our results are in agreement of the Sarma's methodology, who considers a new mechanism for the magnetic interactions responsible for the magnetism on the  $A_2FeMoO_6$  family. We also calculate the cell dimensions that minimize the total energy for each configuration using the Murnaghan equation state.

Keywords: Electronic structure; Half metallic; Complex Perovskite

### **I. INTRODUCTION**

There are currently immense research interests in perovskite oxide materials, because of their varied structure, composition and physical characteristics. These materials have attracted intense research activities in many applied and fundamental areas of solid state science and advanced materials research due the exotic properties such as high temperature superconductivity [1], colossal magnetoresistance [2], half-metallicity [3] and magnetodielectricity [4]. The complex perovskite oxides generally have the formula  $A_2BB'O_6$  and result from the ordering of B and B' cations on the octahedral site of the primitive perovskite unit cell. Magnetic complex perovskites  $A_2BB'O_6$ , with A being alkaline earth ion and B, B' transition metal ions, were discovered by Longo and Ward in 1960's [5]. However, the half-metallic feature of the  $Sr_2FeMoO_6$  was established by Kobayashi et al in 1998 [3]. This exotic property is characterized by the differentiated conducting response of the spin up and spin down orientations. The density of states as a function of energy clearly evidences that majority spin component shows a energy gap at the Fermi level, as the insulating materials, and the other spin orientation is continuous at the Fermi level, due the strong hybridization of Fe  $3d(t_{2g})$  and O  $2p$  states. Moreover, it was experimentally observed that the  $A_2FeMoO_6$  (A=Sr, Ba, Ca), compounds exhibit tunneling magnetoresistance and high Curie temperatures ( $\sim 450$  K) [6]. The extensive half-metallicity studies in double perovskite materials are related with the probable technological applications in *spintronic* devices, such as spin valves, sources for spin polarized electrons and magnetic information storage systems.

*Ab initio* study of disorder effect by band-structure methods was recently reported [7]. Authors used the linear muffin-tin

orbital method within the framework of atomic sphere approximation, finding that disordering destroys the half-metallic nature and leads to a reduction in the net magnetic moment of the ordered system. Studies of self interaction local spin density electronic structure and total energy calculations were performed in  $Sr_2FeMoO_6$  [8]. Their results evidenced a similar electronic structure for A=Sr, Ba and Ca, with a gap energy for the majority spin component and strongly hybridized bands for the minority spin orientation at the Fermi level. The origin of the magnetism in the double perovskites  $A_2FeMoO_6$  evens this in discussion. Recently a new mechanism had been proposed by Sarma [9], in this, the hopping interactions and the hybridization of  $3dMo$  levels and  $2pO$  levels with the  $3dFe$  levels, gives as result, the half-metallic behavior.

In order to analyze the importance of the exchange gap for the half-metallic behavior, in this paper we report a complete electronic-structure analysis by using the Density Functional Theory and the Full Potential Linearized Augmented Plane Waves (DFT-FP-LAPW) method for  $A_2FeMoO_6$  (A=Ba, Ca) compounds. We also calculate the cell dimensions that minimize the total energy for each configuration using the Murnaghan Equation State. Density of states for up and down spin orientations were calculated for the  $t_{2g}$  and  $e_g$  levels of the Fe and Mo elements.

### **II. CALCULATION METHOD**

The calculation of band- and electronic-structure for the complex perovskite  $A_2FeMoO_6$  can be to seen as a many body problem of ions and electrons. The calculations are performed by employing the FP-LAPW method, in the framework of DFT and implemented in the WIEN97 code [10,11]. The FP-LAPW consists in the calculation of solutions for the

Kohn-Sham by the first principles method. In the calculations reported here, we use a parameter  $R_{MT}K_{max}=8$ , which determines matrix size (convergence), where  $K_{max}$  is the plane wave cut-off and  $R_{MT}$  is the smallest of all atomic sphere radii. We have chosen the muffin-tin radii (MT) for Ba, Ca, Fe, Mo and O to be 2.0, 2.0, 1.8, 1.8 and 1.8, respectively.

The exchange and correlation effects were treated by using the Generalized Gradient Approximation (GGA) [12]. This potential considers the difference between the electronic densities for the two distinct spin orientations from the beginning. The density of states is calculated by the histogram method and the position of the Fermi level is found by integrating over the density of states for both spin orientations. The self-consistent calculations are considered to be convergent when the total energies of two successive iterations agreed to within  $10^{-4}$  Ry. We adjusted the Fermi energy to zero. The integrals over the irreducible Brillouin zone are performed up to 47  $\mathbf{k}$ -points.

### III. RESULTS AND DISCUSSION

The tolerance factor ( $f$ ) determines the perovskite structure from the ionic radii of constituted elements of compound, their expression is

$$f = \frac{r_A + r_O}{\sqrt{2}(\langle r_B \rangle + r_O)}, \quad (1)$$

where,  $\langle r_B \rangle$  are the average ionic radius for the ions on the B and B' sites,  $r_A$  is the ionic radii for the ion on the A site and  $r_O$  is the ionic radii of the oxygen. Experimental lattice parameters, tolerance factor and structure type are presented in table I.

TABLE I: Structural parameters for the compound  $A_2\text{FeMoO}_6$  (A=Ba, Ca) [13].

| Compound     | $\text{Ba}_2\text{FeMoO}_6$ | $\text{Ca}_2\text{FeMoO}_6$                                  |
|--------------|-----------------------------|--|
| $f$          | 1.04                        | 0.95   |
| Structure    | Cubic                       | Monoclinic   |
| Exp. Param.  | $a=8.06 \text{ \AA}$        | $a=5.41 \text{ \AA}, b=5.52 \text{ \AA}, c=7.71 \text{ \AA}$ |
| Optimal Par. | $a=8.12 \text{ \AA}$        | $a=5.19 \text{ \AA}, b=5.28 \text{ \AA}, c=7.10 \text{ \AA}$ |

In order to obtain the optimal lattice parameters (table I), corresponding to the minimal energy value, the total energy as a function of volume for the  $\text{Ba}_2\text{FeMoO}_6$  and  $\text{Ca}_2\text{FeMoO}_6$  compounds were determined by fittings with the equation state of Murnaghan. In the case of  $\text{Ca}_2\text{FeMoO}_6$ , with monoclinic structure, we use the experimental ratios  $b/a = 1.02$  and  $c/a = 1.37$ .

As shown in Figs. 1 and 2, for the total density of states close the Fermi level, we observe the same half-metallic nature for both compounds: the spin down channel has a conducting behavior while the spin up evidences an isolated feature. In particular, for the spin up orientation the result for  $\text{Ba}_2\text{FeMoO}_6$  compound evidences occupied states which are

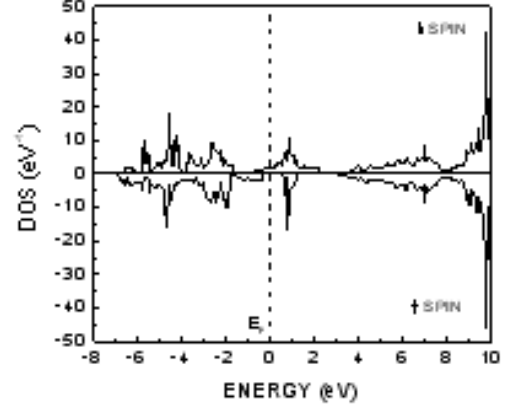


FIG. 1: Total density of states for spin down (above) and up (below) configurations, on the  $\text{Ba}_2\text{FeMoO}_6$  compound.

presented between -8.0 eV to -0.3 eV separated of the unoccupied states by a 0.98 eV gap. For  $\text{Ca}_2\text{FeMoO}_6$  compound, the occupied states with spin up orientation are separated of the unoccupied states by a 0.6 eV gap. This is the reason because this spin channel exhibits an insulating response. In Figs. 3 and 5 we show partial states corresponding to Fe 3d. Partial states corresponding to Mo 4d are shown in Figs. 4 and 6. For the spin down orientation we clearly observe that Mo 4d states contribute to the conducting behavior.

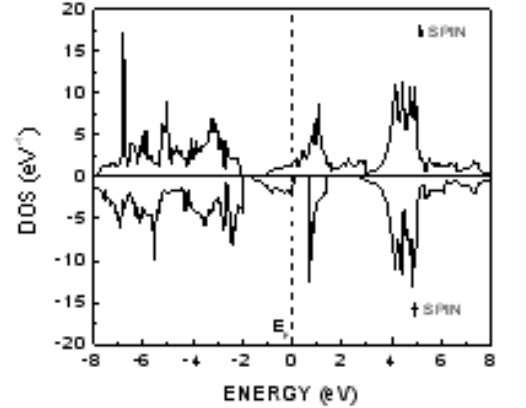


FIG. 2: Total density of states for spin down (above) and up (below) configurations, on the  $\text{Ca}_2\text{FeMoO}_6$  compound.

Fe 3d states are also present, but in a minority proportion. In figures, solid line identifies the delocalized  $d - e_g$  and dot line corresponds to localized  $d - t_{2g}$  states. Fig. 3 shows the partial density of states for both spin orientation, up and down, corresponding to the Fe 3d levels for  $\text{Ba}_2\text{FeMoO}_6$  compound.

It is observed that the crystalline field evidences a splitting

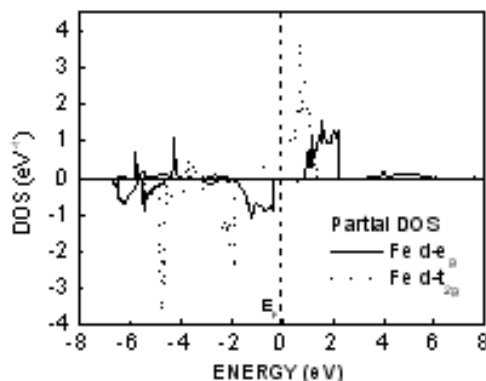


FIG. 3: Partial density of states for spin down (above) and up (below) configurations, for 3d-Fe levels on the  $\text{Ba}_2\text{FeMoO}_6$  compound.

between  $t_{2g}$  and  $e_g$  levels. Exchange splitting between  $t_{2g}$  up and  $t_{2g}$  down, and between  $e_g$  up and  $e_g$  down are also observed. There is a minimal gap of 0.05 eV between  $t_{2g}$  and  $e_g$  levels for the spin down configuration. For the spin up configuration, there is a gap of 0.18 eV between  $t_{2g}$  and  $e_g$  levels. In general, the contribution of  $t_{2g}$  states to DOS is significantly longer than  $e_g$  states for both spin orientations.

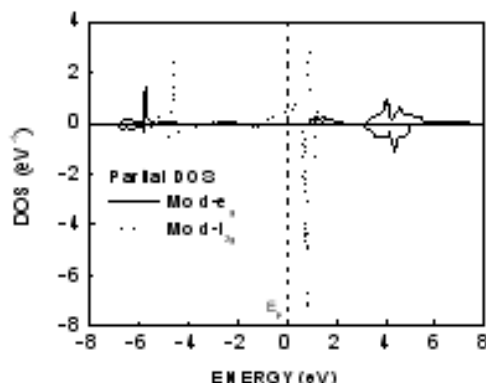


FIG. 4: Partial density of states for spin down (above) and up (below) configurations, for 4d-Mo levels on the  $\text{Ba}_2\text{FeMoO}_6$  compound.

In Fig. 4, we clearly observed the superposition of partial density of states for localized Mo  $d-t_{2g}$  and delocalized Mo  $d-e_g$  levels, which characterize the splitting of crystalline field between  $t_{2g}$  and  $e_g$  states, and exchange splitting between  $t_{2g}$  up and  $t_{2g}$  down levels, and between  $e_g$  up and  $e_g$  down states. There are gaps of 1.92 eV and 2.04 eV between  $t_{2g}$  and  $e_g$  levels for the spin up and spin down configurations, respectively. In this figure, the  $e_g$  levels appear from 3.10 until 6.13 eV.

Figures 5 and 6 describe the exchange and crystalline field

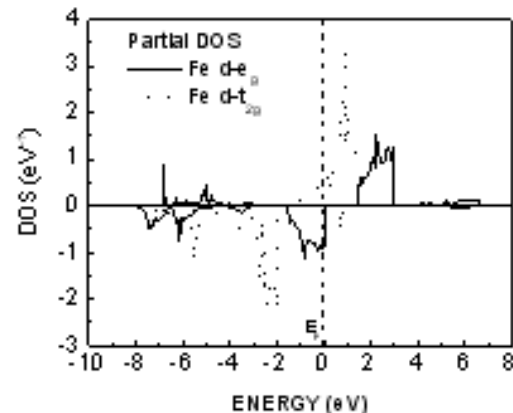


FIG. 5: Partial density of states for spin down (above) and up (below) configurations, for 3d-Fe levels on the  $\text{Ca}_2\text{FeMoO}_6$  compound.

splitting behaviors of Fe 3d and Mo 4d levels, respectively, for the  $\text{Ca}_2\text{FeMoO}_6$  compound. Figure 5 shows a similar behavior for Fe 3d levels with the compound with  $A=\text{Ba}$ , but in this case the gap between the  $t_{2g}$  and  $e_g$  states for the spin up orientation is 0.10 eV and the gap for the  $t_{2g}$  and  $e_g$  states (crystal field) with spin down orientation is 0.38 eV. As in the  $A=\text{Ba}$  case, the main presence of  $t_{2g}$  states is a relevant characteristic in the DOS. Figure 6 shows a similar behavior for Mo 4d levels, with gaps of 2.40 eV and 2.60 eV between  $t_{2g}$  and  $e_g$  states (crystal field) for spin up and spin down orientation, respectively. The  $e_g$  states have high energies between 4.00 eV to 6.80 eV for both spin orientation.

For both compounds the results can be to resume by means the qualitative scheme of figure 7. Part (a) describes the Fe 3d states, where we observe a strong exchange splitting between spin up and spin down for both  $e_g$  and  $t_{2g}$  states. However, the splitting of the crystalline field is relatively weak. The Mo 4d levels are described in part (b) of this diagram. We notice that the  $e_g$  states generally are in higher energy values as compared with Fe states.

Moreover, in the case of Mo levels, the exchange splitting is not observable, due the superposition between  $t_{2g}$  levels for spin up and spin down configuration, while the crystal field is bigger. In part (c) of scheme, according with the Sarma model [9], hopping interactions are responsible for the hybridization of Fe 3d and Mo 4d states. More relevant is the fact that the delocalized  $t_{2g}$  spin down and spin up states are displaced below the Fermi level. However,  $t_{2g}$  spin up states are closer to the Fermi level. As proposed by Sarma [9], the shift of the up- and down-spin states, induce a spin-polarization of the mobile electrons due to hopping interactions between the localized electrons and the conduction states. On the other hand, for both spin orientations up and down,  $e_g$  states are relatively pushed down as a result of the hybridization, but these remain above the Fermi level.

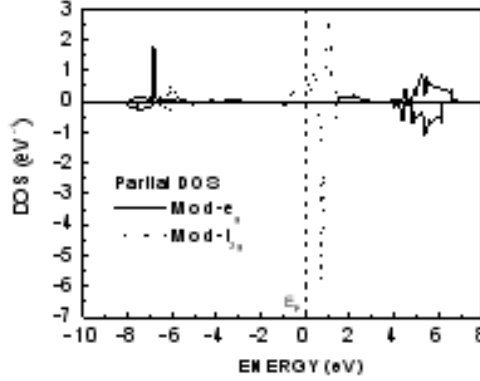


FIG. 6: Partial density of states for spin down (above) and up (below) configurations, for 4d-Mo levels on the  $\text{Ca}_2\text{FeMoO}_6$  compound.

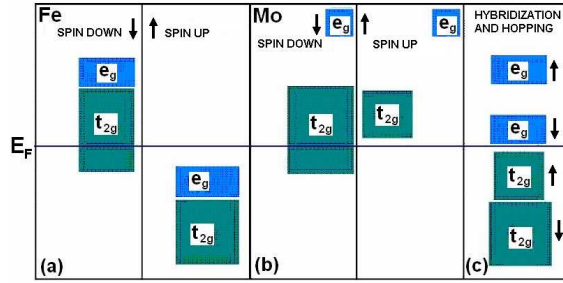


FIG. 7: Qualitative scheme of crystalline field splitting and exchange splitting as a function of energy for: (a) Fe states, (b) Mo states and (c) hybridization of Fe and Mo by considering the hopping interactions.

#### IV. CONCLUSIONS

We perform several *ab initio* calculations over the  $\text{A}_2\text{FeMoO}_6$  ( $\text{A}=\text{Ba}, \text{Ca}$ ) double perovskite. Our results show that it has an insulator behavior for the spin up orientation and conductor for the other one, as expected for half metallic materials. Analysis of electronic structure for  $\text{Ba}_2\text{FeMoO}_6$  and  $\text{Ca}_2\text{FeMoO}_6$  by means calculations of density of states for both spin orientations, based on the DFT-LAPW method permitted to infer that the  $t_{2g}$  spin down states are responsible by the conductivity feature for both Fe 3d and Mo 4d states. On the other hand, the insulate behavior of the spin up configuration can be attributed to the  $e_g$  states.

Additionally, we correlated our results with the recent model propose to explain the conduction mechanism in this kind of compound, by an extension of the methodology of Sarma [9], who considers a new mechanism for the magnetic interactions responsible for the magnetism on the  $\text{A}_2\text{FeMoO}_6$  family. This is performed by using the partial densities of states. We have found that both structures  $\text{Ba}_2\text{FeMoO}_6$  and  $\text{Ca}_2\text{FeMoO}_6$  have half-metallic behavior at the ground state. We also calculate the cell dimensions that minimize the total energy for each configuration using the Murnaghan equation state.

#### Acknowledgements

This work was partially supported by the COLCIENCIAS Colombian agency on the projects 1101-05-13604 and 1101-06-17622. A significant support was furnished by the New Materials Excellence Center, contract 043-2005.

- [1] S. N. Putilin, E. V. Antipov, O. Chmaissem, and M. Marezio, *Nature* **362**, 226 (1993).
- [2] S. Jin, T. H. Tiefel, M. McCormack, R. A. Fastacht, R. Ramesh, and L. H. Chen, *Science* **264**, 413 (1994).
- [3] K. I. Kobayashi, T. Kimura, H. Sawada, K. Tekura, and Y. Tokura, *Nature* **395**, 677 (1998).
- [4] C. Zhong, J. Fang, and Q. Jiang, *J. Phys. Condens. Matter* **16**, 9059 (2005).
- [5] J. M. Longo, R. Ward, *J. Am. Chem. Soc.* **83**, 1088 (1961).
- [6] R. P. Borges, R. M. Thomas, C. Cullinan, J. M. D. Coey, R. Suryanarayanan, L. Ben-Dor, L. Pinsard-Gaudart, and A. Revcolevschi, *J. Phys. Condens. Matter* **11**, L445 (1999).
- [7] T. Saha-Dasgupta, D. D. Sarma, *Phys. Rev. B* **64**, 408 (2001).
- [8] Z. Szotek, W. M. Temmerman, A. Svane, L. Petit, and H. Win-

ter, *Phys. Rev. B* **68**, 104411 (2003).

- [9] D. D. Sarma, Sugata Ray, *Chem. Sci.* **113**, 515 (2001).
- [10] D. J. Sing, *Plane waves pseudo-potentials and the LAPW method*, Kluwer Acad. 1994.
- [11] P. Blaha, K. Schwarz, and J. Luitz. WIEN 97. *A Full Potential Linearized Augmented Plane Wave Package for Calculating Crystal Properties*. Katherine Schwarz, Tch. Universität Wien, Austria., 1999.
- [12] J. P. Perdew, K. Burke, and M. Ernzerhof, *Phys. Rev. Lett.* **77**, 3865 (1996).
- [13] J. B. Philipp, P. Majewski, L. Alff, et al. *Cond. Matt.* **30**, 2360, (2003).